Ionic Conduction in Polyphosphazene Solids and Gels: ^{13}C, ^{31}P, and ^{15}N NMR Spectroscopy and Molecular Dynamics Simulations

Harry R. Allcock,* Mark E. Napierala, David L. Olmeijer, Scott A. Best, and Kenneth M. Merz, Jr.*

Department of Chemistry, The Pennsylvania State University, University Park, Pennsylvania 16802

Received April 24, 1998

ABSTRACT: Polyphosphazene single-substituent polymers were synthesized with the general formula $[NP(OCH_2CH_2OCH_2CH_2XCH_3)_2]$ where X = oxygen for polymer **5** or X = sulfur for polymer **6**. Characterization of these materials made use of ^1H, ^{13}C, ^{15}N, and ^{31}P nuclear magnetic resonance (NMR) spectroscopy, differential scanning calorimetry, gel permeation chromatography, and elemental microanalysis. The polymers were complexed with $LiSO_3CF_3$ and $AgSO_3CF_3$ and examined both as solid electrolyte media and in the presence of dimethylformamide solvent. The ionic conductivities of these materials were determined at 25 °C through the use of complex impedance analysis. The mechanism of ionic conduction in the polymer−salt complexes was probed through an examination of ^{13}C, ^{31}P, and ^{15}N NMR shifts and ^{13}C NMR spin−lattice relaxation times (T_1) for d_7-DMF solutions. Molecular dynamics simulations were also carried out in order to investigate the interactions within the polymer−salt−DMF complexes.

Introduction

The discovery that salts dissolved in solid polymeric materials can act as ionically conducting media was made more than 20 years ago. Wright first reported the ability of poly(ethylene oxide) (PEO) to dissolve alkali metal salts such as sodium and potassium thiocyanates and for the mixtures to conduct electricity by an ionic process.[1] Later, Armand demonstrated that PEO−salt complexes can be used as a solid solvent in ionically conducting, rechargeable, lithium batteries.[2] This discovery stimulated numerous investigations of PEO, as well as other polymers, for this application.

A number of subsequent studies revealed various characteristics that a polymer must possess if it is to be used as a solid electrolyte medium.[3−5] First, the polymer must be noncrystalline. Ionic conduction occurs through the amorphous regions of a polymer. Second, the polymer must possess coordination sites for cations or anions to aid in the dissolution and ion-pair separation of the salt. Third, the polymer should be flexible at the molecular level. This flexibility, which is associated with a low glass transition temperature (T_g), allows sufficient segmental motion for the facile migration of ions through the solid electrolyte medium.

In view of these criteria, a class of promising materials for use as polymer electrolytes are the polyphosphazenes. Polyphosphazenes are macromolecules of formula $(NPR_2)_n$ with a highly flexible backbone of alternating nitrogen and phosphorus atoms. The ease of torsion about the nitrogen−phosphorus bonds can yield polymers with some of lowest T_g's known (−80 to −100 °C). The side groups, R, include alkyl, aryl, alkoxy, aryloxy, or amino substituents, each of which will generate polymers with different materials properties.[6−8] Several hundred different polyphosphazenes are known.

The first polyphosphazene shown to give ionic conductivity when complexed with a metal salt was poly[bis(2-(2-methoxyethoxy)ethoxy)phosphazene], MEEP (structure **1,** where X = oxygen**)**).[9−13] This material, with dissolved lithium or silver triflate, has an ionic conductivity in the range of 10^{-5} S/cm, which is 2−3 orders of magnitude higher than PEO lithium triflate complexes at room temperature. Recently, other related polyphosphazenes have been synthesized, and some of these demonstrate higher conductivities, as well as increased dimensional stability.[14]

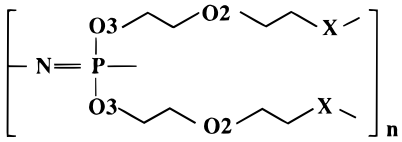

X = O1 or S1

1

Parallel with this work on solid polymer electrolytes has been the technological development of "gel" battery electrolytes in which polymer molecules and salts are dissolved in an organic solvent. These generate higher conductivities (up to 10^{-3} S/cm) but suffer from the possibility of liquid leakage when damaged and from a fire hazard. Recent work in our program has drawn attention to the advantages of polyphosphazenes that contain small amounts of organic solvents as 10^{-3} S/cm level electrolytes.[15]

A crucial need in the development of both types of polymer electrolyte media is an understanding of the interactions between the host polymer or the solvent and the ions and to relate this to the ionic conductivities. Attempts to explain the mechanism of ionic conduction for solid polymer−salt complexes have been made based on information provided by the measurement of transport numbers, infrared and Raman spectroscopy, various NMR spectroscopic techniques, and molecular modeling.[16−23] These studies have been performed mainly on PEO.[24−26] The mechanism of ionic conduction in polyphosphazenes is only partly understood. Moreover, information determined for PEO may not be directly applicable to a polyphosphazene because of the structural and morphological differences between these systems. Hence, in this work an attempt has been made to probe the nature of cation coordination to specifically

10.1021/ma980665+ CCC: $18.00
Published on Web 01/16/1999

Scheme 1. Synthesis of (2-(2-Methylthio)ethoxy)-ethanol

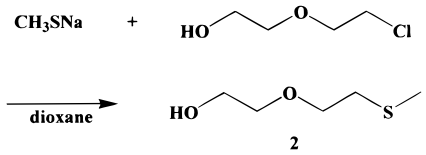

2

Scheme 2. Synthesis of Polymers 5 and 6

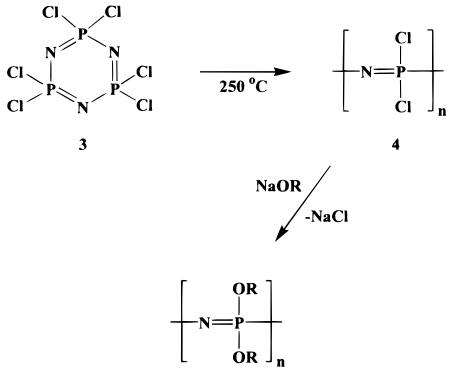

OR	polymer
$OCH_2CH_2OCH_2CH_2OCH_3$	5
$OCH_2CH_2OCH_2CH_2SCH_3$	6

tailored polyphosphazenes, especially in systems that contain an organic solvent.

The first objective was to examine the role played by different coordination sites on the polymer and to attempt to correlate this with the conductivity of a polyphosphazene. Studies with solid PEO−salt complexes have shown that a direct interaction exists between the lone pair electrons of the etheric oxygen atoms and metal ions.[27] It is believed that this interaction is the underlying factor responsible for ionic conductivity in these systems. In the work reported here, oxygen as well as sulfur coordination sites within the side chains of the phosphazene polymers were examined. Polymer **5** contained only oxygen coordination sites while polymer **6** contained both sulfur and oxygen atoms.

The second objective was to investigate the interactions of the synthesized polymers with lithium and silver ions. These interactions were studied through ^{13}C, ^{31}P, and natural abundance ^{15}N NMR spectroscopy, as well as ^{13}C NMR spin−lattice relaxation times (T_1's) and molecular dynamics (MD) simulations.

Finally, an attempt was made to examine the ability of the polymers to coordinate to cations in the presence of a coordinative small-molecule solvent such as dimethylformamide (DMF). This aspect is relevant to the design of "gel" electrolytes, which are currently of considerable practical interest.

Results and Discussion

Polymer Synthesis and Characterization. The assembly of the side groups used in polymer **6** is shown in Scheme 1. The syntheses of polymers **5** and **6** were carried out as shown in Scheme 2. The side group alcohol was allowed to react with a slight excess of sodium metal in tetrahydrofuran. To this mixture was then added dropwise poly(dichlorophosphazene) (**4**) in tetrahydrofuran. This order of addition was used to maintain an excess of the side group reagent in the reaction medium. The structure of each polymer was verified by ^1H, ^{13}C, ^{15}N, and ^{31}P NMR spectroscopy, DSC, GPC, and elemental analysis. All the NMR spectra were consistent with the theoretical values for pure polymers, and the elemental analyses detected only very small amounts of residual chlorine (<216 ppm) for both macromolecules. This indicates that the replacement of the chlorine atoms by the alkoxy units was essentially complete.

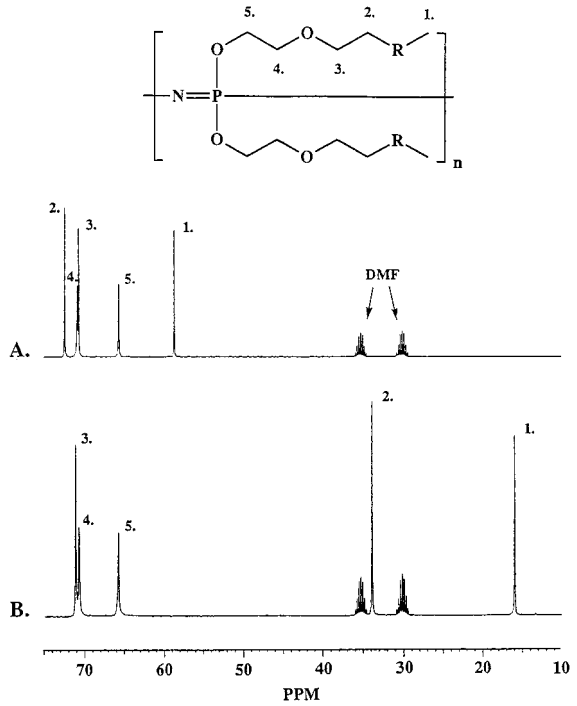

Figure 1. Carbon peak assignments for polymers **5** and **6**.

Table 1. Spin−Lattice Relaxation Times (T_1) for Polymers 5 and 6 (25 °C, Seconds)

polymer	C1	C2	C3	C4	C5
5	5.05	1.44	0.95	0.38	0.31
6	5.34	0.99	0.76	0.30	0.29

^{13}C Assignment of Polymers. The ^{13}C NMR peak assignments for solutions of polymers **5** and **6** in DMF are shown in Figure 1. They were determined through various NMR techniques which included one-dimensional homonuclear ^1H decoupling experiments, two-dimensional $^{13}C-^1H$ correlations, and ^{13}C spin−lattice relaxation, T_1, experiments. Carbons 1, 2, and 5 were assigned with the use of ^1H decoupling experiments followed by two-dimensional $^{13}C-^1H$ correlations. Carbons 3 and 4 were assigned through the use of T_1 experiments (Table 1), since the two-dimensional procedures led to ambiguous peaks for these carbon atoms. It is known that carbon atoms that are further from the polymer backbone in a flexible side chain will have longer relaxation times because of their increased mobility.[28] Thus, for polymer **5**, the peak at 70.69 ppm with a relaxation time of 0.95 s was assigned to carbon 3, and the peak at 70.85 ppm with a relaxation time of 0.38 s was assigned to C4. For polymer **6** the peak at 71.06 ppm with a relaxation time of 0.76 s was assigned to C3, and the peak at 70.64 ppm with a relaxation time of 0.30 s was assigned to C4.

Polymer−Salt Complexes. The following solutions were each prepared at five salt concentrations that varied from 0 to 43.7 mol %: polymer **5** with $LiSO_3CF_3$,

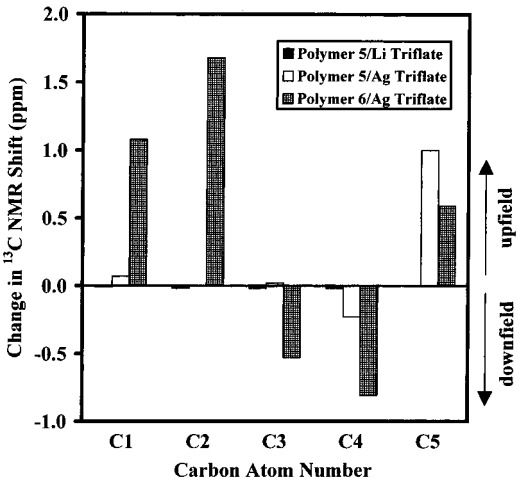

Figure 2. Change in ^{13}C NMR shifts for polymers **5** and **6** in d_7-DMF after salt complexation.

polymer **5** with $AgSO_3CF_3$, and polymer **6** with $AgSO_3CF_3$. These mixtures were then dissolved in d_7-DMF. Polymer **6** complexed with $LiSO_3CF_3$ could not be prepared at concentrations above 0.5 M of **6** in d_7-DMF. At higher concentrations a precipitate formed which presumably consisted of the macromolecule complexed with the salt. An attempt was made to measure ^{13}C and ^{31}P NMR shifts for 0.5 M solutions of polymers **5** and **6** in d_7-DMF with both salts. However, no appreciable ^{13}C shift changes with increasing salt concentration were detected in this concentration range. This suggests that, at this dilution, polymer−salt complexation is overwhelmed by the interactions of the ions with DMF. For this reason, 1 M polymer solutions were examined, in which the concentration and therefore the ion-complexing behavior of the d_7-DMF solvent were sufficiently low that it did not interfere completely with all the polymer−salt interactions.

^{13}C, ^{31}P, and ^{15}N Natural Abundance NMR Results. The ^{13}C NMR shifts were examined for the polymers in d_7-DMF. The change in these shifts, following polymer complexation with the lithium or silver salts, is shown in Figure 2. (Only the data obtained for the highest concentrations of $LiSO_3CF_3$ or $AgSO_3CF_3$ are included in Figure 2. In general, if a change in the ^{13}C NMR chemical shift was detected at all, its magnitude increased with increasing salt concentration.) Polymer **5** complexed with 43.7 mol % $LiSO_3CF_3$ showed little or no change in ^{13}C chemical shift for any of the carbon atoms. This result does not necessarily imply that polymer **5** is a poor solvation donor for lithium ions. It is known that lithium will interact preferentially with DMF rather than with polymeric etheric oxygen atoms.[29] The coordinative interactions between the lithium ions and a solvent such as DMF depend on the dielectric constant and donor number of the solvent.[30] DMF has the ability to solvate alkali metal ions rather well, possessing a Gutmann donor number of 26.6.[31] Moreover, it has a moderate dielectric constant of 36.7. These values indicate that DMF will act as a good solvator, will reduce the number of tight ion pairs, and will coordinate with the lithium ions in the form of solvent-separated ion pairs or free solvated ions. Because of these interactions, DMF probably competes effectively for lithium ions, the polymer−salt interactions are limited, and only small chemical shifts would be expected for the carbon atoms in the polymer.

For polymer **5** complexed with 31.8 mol % $AgSO_3CF_3$ and dissolved in d_7-DMF, appreciable chemical shifts of 0.23 and 1.00 ppm were detected for C4 and C5, respectively (these are the carbons closest to the skeleton). The ability of silver ions to complex more readily than lithium ions with the polymer can be explained if the system is considered to be a competitive solvent mixture of polymer and DMF. It is believed that cations of high charge density prefer the more basic solvent in a mixture.[32] Thus, lithium ions prefer to interact with DMF. However, the charge density of silver is smaller than that of lithium, allowing it to interact with the etheric components of the polymer as well.

Because C4 and C5 of polymer **5** complexed with $AgSO_3CF_3$ give the largest chemical shifts, a superficial analysis might suggest that the silver ions are preferentially coordinated to either the oxygen atom closest to the polymer backbone or the nitrogen atoms in the backbone. The direction of the shift change for C4 is upfield and that of C5 is downfield. However, the complexity of this system is such that this conclusion may be an oversimplification. Previous studies on small donor molecules, such as cyclic ethers, indicated that either downfield or upfield shifts for carbon atoms depend on the solvent concentration, the ion examined, and the size of the donor atom molecules.[33−37] Thus, we conclude that polymer **5** interacts with Ag^+ more strongly than with Li^+ in the presence of DMF, but the exact site of interaction with Ag^+ is not clear.

Complexes of polymer **6** with 34.4 mol % $AgSO_3CF_3$ showed ^{13}C NMR peak shifts for all five carbon atoms. Atoms C1 and C2 gave the largest shifts, with changes of 1.48 and 1.68 ppm downfield, respectively. This may indicate a preferential interaction of silver ions with the sulfur atoms in the polymer side chain. Previous studies on linear and cyclic species that contain sulfur support this view.[38,39] Atoms C3 and C4 were shifted upfield, with changes of 0.53 and 0.81 ppm, respectively. C5 had a downfield shift of 0.54 ppm. These shift changes are not definitive, but they may indicate that both of the oxygen atoms in a polymer side chain are coordinated to silver, although probably not to as great an extent as the sulfur atoms.

As discussed, a similar experiment could not be carried out on complexes of polymer **6** with $LiSO_3CF_3$. One study that examined sulfur-containing macrocycles and alkali metal ions found little or no interaction between the two species.[40] However, polymer **6** in the presence of $LiSO_3CF_3$ precipitates at a 1 M concentration of polymer and 0.9 M concentration of $LiSO_3CF_3$. DMF is probably involved through electrostatic interactions, since this complex solvates on heating and reprecipitates following cooling.

An attempt was also made to detect an interaction between metal cations and the lone pair electrons of the backbone nitrogen atoms in polymers **5** and **6**. ^{31}P and ^{15}N natural abundance NMR spectra were obtained for 1 M polymer solutions in d_7-DMF with varying salt concentrations. An interaction between the metal ion and the backbone nitrogen atoms should give rise to a shift in signal of both the phosphorus and nitrogen nuclei as the amount of salt is increased. The results for the ^{31}P NMR shifts can be seen in Figure 3.

The largest shift in the ^{31}P NMR spectrum is a downfield shift of 4.42 ppm for polymer **5** when complexed with 31.8 mol % $AgSO_3CF_3$ in d_7-DMF. A 2.16 ppm downfield shift of the ^{31}P NMR peak was detected

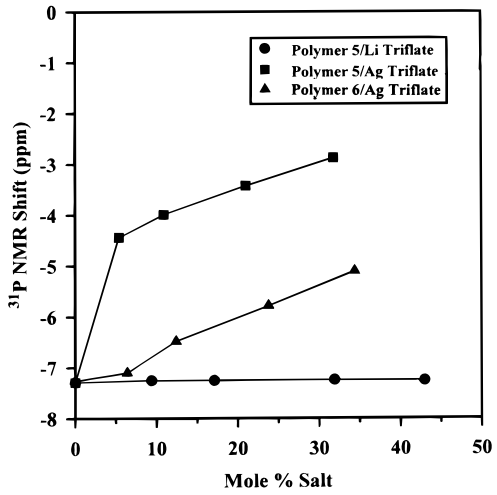

Figure 3. Change in ^{31}P NMR shifts for polymers **5** and **6** in d_7-DMF after salt complexation.

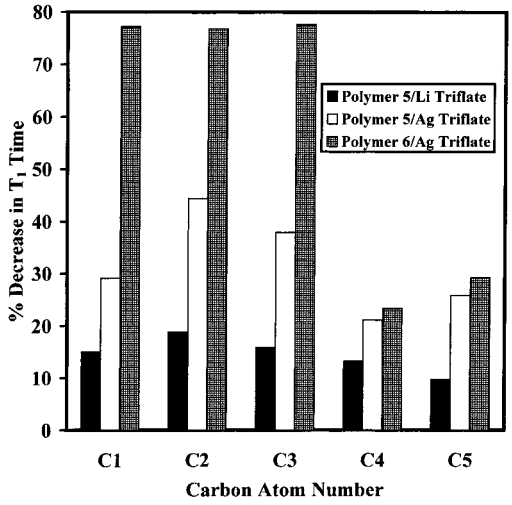

Figure 4. Decrease in ^{13}C NMR T_1 times for polymers **5** and **6** in d_7-DMF after salt complexation.

for polymer **6** when complexed in the presence of 34.4 mol % $AgSO_3CF_3$. It appears that silver ions can indirectly withdraw electron density from the skeletal phosphorus atoms, thus deshielding phosphorus and shifting the signal downfield. No appreciable change in the ^{31}P NMR spectrum was detected for polymer **5** in the presence of $LiSO_3CF_3$ (0.04 ppm), even at the highest salt concentrations used. This again implies that the interaction between the DMF solvent molecules and *lithium* cations is greater than the polymer−lithium interactions. However, this is not the case for the *silver* cations, whose interactions with the polymer are not appreciably disrupted by the presence of the highly polar DMF solvent molecules. Thus, these results are consistent with the ^{13}C NMR data.

^{15}N natural abundance NMR (the natural abundance of ^{15}N is 0.36%[41]) was also utilized to investigate if coordination of the metal cations to the backbone nitrogen atoms occurred. The results indicated that no appreciable ^{15}N NMR shift occurred as the amount of salt in the system was increased. (The largest observed shift for any system was a 0.4 ppm downfield shift for the ^{15}N NMR peak of polymer **6** complexed with 34.4 mol % $AgSO_3CF_3$.) This implies that the cations do not coordinate to these nitrogen atoms.

^{13}C NMR Relaxation Times. Another approach used to investigate the involvement of individual polymer side-chain coordination sites was via the study of the ^{13}C spin−lattice relaxation times, T_1. This method has some advantages over an examination of ^{13}C shifts for complexed materials. Competing electrostatic interactions, together with uncertainty about preferred conformational changes, make the interpretation of ^{13}C shift data difficult. However, for NMR relaxation data, the local microscopic magnetic field is affected to a lesser degree by these interactions. Relaxation data for salt-free polymers **5** and **6** are shown in Table 1. An increase in T_1 occurs the further the carbon atom is located away from the polymer backbone. For example, C5 for polymer **5** has a T_1 of 0.31 s and C1 has a T_1 of 5.05 s. This suggests an increase in the mobility of the atoms (i.e., a higher number of degrees of rotation) at increasing distances from the polymer backbone. A similar result has been found in other systems.[28]

However, this technique is not without its shortcomings. The T_1 times for *all* carbon atoms for both polymers decreased following the addition of salt. This could be an indication that the local environment of a carbon atom has changed, presumably the result of metal ions coordinating to oxygen atoms that are directly bonded to the carbon atoms of interest. However, the addition of salt also increases the viscosity of the solvent medium. This in turn will cause a decrease in the mobility of the carbon atoms, also causing a decrease in the T_1 times as measured by ^{13}C NMR. Thus, care must be taken not to overinterpret the T_1 data.

The percent decrease in T_1 times for the polymers was calculated following salt complexation. These results are included in Figure 4. (Once again, only the data obtained for the highest concentrations of $LiSO_3CF_3$ or $AgSO_3CF_3$ are included in this figure. In all cases, the change in T_1 was greater with increasing salt concentration.) Polymer **5** complexed with $LiSO_3CF_3$ showed the smallest change in T_1. Furthermore, no one carbon atom seemed disproportionately affected by the introduction of salt with respect to the others. This again indicates a preferred interaction of the lithium ions with the solvent (DMF) rather than with the etheric side-chain sites of polymer **5**, and it is difficult to attribute the T_1 change to any factor other than an increase in solution viscosity following the addition of salt. A study on a similarly substituted, cross-linked, polysiloxane polymer arrived at the conclusion that the oxygen atom closest to the backbone may play a lesser role in the coordination of lithium ions than do those further from the main chain.[42] However, due to interference by the DMF solvent molecules, no such conclusions could be drawn for polymer **5** with $LiSO_3CF_3$ in DMF based on either the ^{13}C NMR chemical shift or relaxation time data.

At the other extreme, the largest changes in T_1 values were for polymer **6** after complexation with $AgSO_3CF_3$, as shown in Figure 4. Furthermore, the change in T_1 affects different carbon atoms disproportionately. In this complex, C1, C2, and C3 have 77.2%, 76.8%, and 77.6% decreases in T_1 times, respectively. This reinforces the evidence for a strong interaction of the side group sulfur atom with the silver ion. This is also supported by the change in ^{13}C NMR shifts for the peaks that correspond to C1 and C2 of this polymer following salt complexation. The decreases in T_1 times for atoms C4 and C5 (23.3% and 29.2%, respectively) are much smaller than those for C1−C3, and this may simply be due to the

Table 2. Concentration of Ions in Model Polymers 7 and 8[a]

polymer model	no. of metal cations	no. of triflate anions
7	9 Li^+	9 OTf^-
7	5 Ag^+	5 OTf^-
8	5 Ag^+	5 OTf^-

[a] All three models were run in the presence of solvent as well as without solvent molecules.

increased solution viscosity from the increasing salt concentration. However, because the T_1 time changes are greater here than for any of the other polymer/salt systems, it seems possible that complexation between silver ions and the oxygen atoms does occur, albeit with a smaller magnitude than found for the sulfur atom. The ^{13}C NMR shift data and ^{31}P NMR data both support this impression, that some (weak) complexation occurs between the oxygen atoms and the silver cations.

The two T_1 studies described above are for the extreme cases: (1) where little or no change in the T_1 values occurs or (2) where larger T_1 changes occur which affect certain atoms in the same polymer side chain. The complexation of polymer **5** with $AgSO_3CF_3$ presented an intermediate situation. The percent decreases in the T_1 values of the carbon atoms of this polymer−salt complex are intermediate between the other two sets of data. As discussed, the ^{13}C peak shifts and ^{31}P NMR data of polymer **5**, when complexed with $AgSO_3CF_3$ compared to the analogous $LiSO_3CF_3$ complexes, suggest an increased coordination of the cation to the polymer and a decreased interaction between the metal ion with the DMF solvent molecules. This is partially substantiated by the T_1 data. The T_1 times for all five carbon atoms in the side chains of polymer **5** indicate larger responses to the silver ions than to lithium ions. If any of the carbon T_1 times are affected disproportionately following complexation to the $AgSO_3CF_3$ salt, it appears to be C2 and C3.

It appears that the solvation strength of DMF for the silver ion is similar to that of the etheric side chains of polymer **5**. Thus, the complexes formed by silver ions at more distant locations from the backbone would probably involve both DMF and polymer oxygen atoms. In this case, the silver ion association with both the polymer and DMF molecules may be such that there is no significant change in the ^{13}C NMR shifts.

Molecular Dynamics (MD) Simulations. Molecular dynamics simulations were carried out in order to further investigate the interactions between the metal ions and polymers **5** and **6**. The initial structures for the MD simulations were constructed by placing five polymer chains, each consisting of 10 repeat units, in a dimethylformamide (DMF) solvent box[43] in the presence of either $LiSO_3CF_3$ or $AgSO_3CF_3$. Polymer model **7** was constructed as a model for polymer **5** (with only oxygen coordinating sites on the side chain). Polymer model **8** modeled polymer **6** (with both sulfur and oxygen coordination sites). To make a comparison to the experimental NMR data, three different polymer models were devised: model **7** complexed with $LiSO_3CF_3$, model **7** complexed with $AgSO_3CF_3$, and model **8** complexed with $AgSO_3CF_3$. The number of ions that were included in each simulation was based on the optimal experimental salt concentrations which gave the highest ionic conductivities for the respective polymer−salt complexes (discussed in the last section), and these are shown in Table 2. Initially, the five polymer chains were arranged parallel to each other, thus creating the shape of an X if viewed from above the model. The $LiSO_3CF_3$ and $AgSO_3CF_3$ salt molecules were introduced into the simulation as individual ions (Li^+ or Ag^+ and $SO_3CF_3^-$) with each ion randomly oriented around the polymer chains so as to avoid any undesirable nonbond contacts between the polymer and the ion which might give rise to very large repulsive forces during the course of the simulations. The net charge on the polymer−salt system was zero.

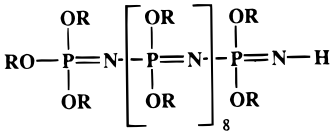

R = $CH_2CH_2OCH_2CH_2OCH_3$ (**7**)
= $CH_2CH_2OCH_2CH_2SCH_3$ (**8**)

Since almost all of the MD studies on polymer electrolytes in the past have focused on PEO[22,23,44,45] rather than polyphosphazenes, some force field development was necessary before MD simulations could be carried out. In calculating atomic partial charges for **7** and **8**, the polymer chain was initially modeled using smaller molecules **9** and **10**, respectively, which are analogous to repeat units in the polymer chain. Smaller structures were required in order to obtain the partial atomic charges since the 10 repeat unit polymer models **7** and **8** were much too large to be modeled quantum mechanically. Structures **9** and **10** were initially optimized using the PM3 Hamiltonian[46,47] in MOPAC 6.0.[48] The partial atomic charges for these molecules were obtained with quantum mechanical electrostatic potential (ESP) fitting using the 6-31G* basis set[49,50] and restrained electrostatic potential fitting.[51] Once the fitting was completed, hydrogen atoms were averaged on each of the methyl and methylene groups in the polymer side chains. These charges were then used for the repeat units in the larger polymer chains. However, a slight positive net charge was calculated when summing the charges for each repeat unit in the larger polymer chains. Having a net charge is undesirable since the experimentally synthesized polymer is neutral. Therefore, slight modifications were made to the atomic partial charges on the phosphorus atoms in the polymer backbone in order to render the total system neutral.[52] The partial atomic charges for the triflate anion were also obtained from quantum mechanical electrostatic potential (ESP) fitting using the 6-31G* basis set[49,50] and restrained electrostatic potential fitting.[51]

Taking into consideration that both polymers **5** and **6** are completely amorphous and have no ordered structures, the starting configurations of the polymer chains were constructed so as to avoid any unacceptable nonbond interactions. The crystal structure of the triflate anion[53] was used as a basis for its ionic structure in solution. The crystal structures of the DMF solvent molecules were also used in all of the models. The MD simulations were carried out using the all-atom AMBER force field with the following additions.[54] Force field parameters for the triflate anion were taken from Lingren et al.[53] while the nonbond parameters for the silver ion were obtained from the work of Laaksonen and Kovacs.[55] Parameters involving atoms in the polymer backbone were obtained from the work of Boyd and Kesner[56] as well as through experimental spectroscopic

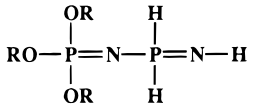

Capping Group (**9**)

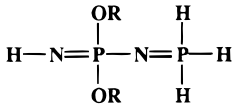

Repeat Units (**10**)

R = $CH_2CH_2OCH_2CH_2OCH_3$ (**7**)
= $CH_2CH_2OCH_2CH_2SCH_3$ (**8**)

data.[7,57] Because both polymers **5** and **6** are highly flexible and have a low T_g, the barrier height for rotation about the polymer backbone was set at 0.01 kcal/mol repeat unit, which essentially allows for free rotation along the polymer backbone.

One of the aims of these simulations was to examine the coordination sites of the Li^+ and Ag^+ ions. Structural features of the models were analyzed by calculating average distances between the metal ions and the various heteroatoms in the polymer chains. The average distances between the metal ions and the triflate anions were also measured in order to determine the extent of ion pairing in the polymers. Since many of the current theories of ion transport in polymer electrolytes, such as PEO, employ mechanisms that involve extensive ion pairing and clustering, these phenomena should also be addressed in order to see whether similar trends exist with the polyphosphazenes.[22,23,44,45] No distances were calculated between the solvent molecules and the metal ions. Structure **1** illustrates the labeling scheme adopted for the heteroatoms in the polymer side chains. The polymer backbone atoms were numbered in numerical order based on the number of the repeat unit (e.g., the first repeat unit is labeled as $(-P1{=}N1-)_n$).

Table 3 lists the average bond distances for polymer **7** complexed with $LiSO_3CF_3$ in DMF. As the data reveal, five Li^+ ions were completely solvated by DMF solvent molecules. Only three Li^+ ions were associated with atoms in the polymer side chains, and in each case, the cation is coordinated to four oxygen atoms on different side groups, oxygens which are located furthest from the polymer backbone. This supports the experimental NMR results obtained for polymer **5** when complexed with $LiSO_3CF_3$ and shown in Figures 2, 3, and 4. Experimentally, there was little or no change in the ^{13}C NMR shifts or T_1 times for the carbon atoms of this polymer−salt complex. Most of the Li^+ ions in the MD simulations are not coordinated to the polymer and therefore would not cause any substantial chemical shift in the ^{13}C signals. The ^{31}P and ^{15}N NMR experimental results also are supported by the MD simulations. Of the three Li^+ ions which are associated with the polymer, none are located near the polymer backbone and therefore would not give rise to any chemical shifts in these spectra.

In changing the metal ion from Li^+ to Ag^+, the simulation results were significantly different. Average bond distances for polymer **7** complexed with $AgSO_3CF_3$ in DMF are given in Table 4. Unlike the Li^+ ions, which were not highly coordinated to the polymers, all five of the silver ions were found to be associated with the polymer structures and are coordinated to either four or six heteroatoms. This general result is, for the most part, substantiated by the experimental NMR data, which show greater coordination of polymer **5** with Ag^+ than with Li^+ in the presence of DMF.

Analysis of the data inTable 4 suggests no preferred binding of the Ag^+ cations to any of the oxygen atoms in the polymer side chains. Moreover, the simulation

Table 3. Calculated Average Bond Distances and Rms Errors between Coordinated Li^+ Ions and the Heteroatoms in Model Polymer 7

Li^+ ion no.	residue no.[a]	coordinated atoms[a]	avg distance (Å)	standard deviation
1	59	O2	2.10	0.12
	63	O1	2.13	0.14
	63	O2	2.16	0.18
	59	O1	2.18	0.17
2	48	O2	2.00	0.09
	44	O1	2.07	0.12
	44	O2	2.09	0.13
	48	O1	2.16	0.20
3	105	O2[b]	2.03	0.12
	47	O2	2.09	0.13
	49	O1	2.14	0.15
	49	O2	2.24	0.15
	47	O1	2.52	0.36
4	*c*	*c*	*c*	*c*
5	*c*	*c*	*c*	*c*
6	52	O1	2.21	0.22
	52	O2	2.56	0.51
7	*c*	*c*	*c*	*c*
8	*c*	*c*	*c*	*c*
9	101	O1[b]	2.28	0.82

[a] Listed are both the residue number and the polymer atom to which the Li^+ ions are coordinated (see Figure 8 for the labeling of the oxygen atoms). Bond distances in which the Li^+ ions are bound to solvent molecules are not given. [b]Triflate ion. [c]No coordination.

Table 4. Calculated Average Bond Distances and Rms Errors between Coordinated Ag^+ Ions and the Heteroatoms in Model Polymer 7

Ag^+ ion no.	residue no.[a]	coordinated atoms[a]	avg distance (Å)	standard deviation
1	55	N1	2.37	0.10
	67	O2	2.37	0.11
	61	O2	2.40	0.12
	61	O1	2.47	0.16
	67	O1	2.52	0.20
	55	N2	2.62	0.18
2	41	O1	2.38	0.12
	38	O2	2.38	0.13
	38	O1	2.43	0.20
	41	O2	2.47	0.19
3	1	N1	2.30	0.09
	8	O2	2.39	0.13
	8	O1	2.46	0.18
	8	O3	2.62	0.25
	1	N2	2.67	0.29
4	19	N1	2.26	0.07
	37	N1	2.30	0.08
	25	O2	2.40	0.16
	25	O1	2.45	0.15
5	76	O2	2.33	0.10
	75	O2	2.35	0.10
	76	O1	2.42	0.14
	75	O3	2.49	0.14
	76	O1	2.53	0.18
	75	O3	2.59	0.17

[a] Listed are both the residue number and the polymer atom to which the Ag^+ ions are coordinated (see Figure 8 for the labeling of the oxygen atoms). Bond distances in which the Ag^+ ions are bound to solvent molecules are not given.

Table 5. Calculated Average Bond Distances and Rms Errors between Coordinated Ag^+ Ions and the Heteroatoms in Model Polymer 8

Ag^+ ion no.	residue no.[a]	coordinated atoms[a]	avg distance (Å)	standard deviation
1	55	N1	2.25	0.06
	67	O2	2.37	0.13
	55	N3	2.39	0.12
	67	S1	2.75	0.15
2	37	N1	2.31	0.08
	45	O2	2.37	0.12
	42	O2	2.40	0.12
	37	N2	2.41	0.10
	45	O3	2.45	0.15
	42	O3	2.54	0.15
3	1	N1	2.25	0.06
	8	O2	2.32	0.10
	1	N3	2.35	0.08
	8	O3	2.55	0.19
	1	N2	2.69	0.17
	8	S1	2.80	0.20
4	19	N1	2.24	0.06
	37	N1	2.28	0.07
	38	O2	2.39	0.13
	20	O3	2.49	0.17
	38	O3	2.60	0.18
	38	S1	2.80	0.18
5	73	N1	2.26	0.07
	76	O2	2.37	0.11
	73	N3	2.40	0.15
	80	O3	2.60	0.26
	73	N2	2.80	0.24

[a] Listed are both the residue number and the polymer atom to which the Ag^+ ions are coordinated (see Figure 8 for the labeling of the oxygen atoms). Bond distances in which the Ag^+ ions are bound to solvent molecules are not given.

suggests coordination of the Ag^+ ions to the nitrogen atoms in the polymer backbone. This is not consistent with the NMR results for polymer **5** complexed to $AgSO_3CF_3$. As illustrated in Figure 2, the experimental ^{13}C NMR results indicate substantial shifts for those carbon atoms located closest to the polymer backbone and much smaller shifts for the more distant atoms. However, no appreciable shift change was detected in the ^{15}N natural abundance NMR (despite the substantial shift change of the ^{31}P NMR, as shown in Figure 3) following polymer complexation with the salt. Although the simulation data in Table 4 suggest that considerable binding exists between Ag^+ and O2 and O3 (the oxygen atoms closest to the polymer backbone), they also suggest complexation to O1 and to the backbone nitrogen atoms. The MD simulations are more in accord with the experimental T_1 relaxation time experiments.

The third model that was studied was species **8** complexed with $AgSO_3CF_3$ in DMF. Average distances were calculated as described previously and are recorded in Table 5. Of interest in this model is the interaction between the Ag^+ ions and the sulfur atoms (S1) which replaced O1 in the polymer side chains (structure **1**). As with the previous model, the Ag^+ associates preferentially with the polymer rather than with the DMF solvent molecules. The Ag^+ ions appear to be predominantly hexacoordinated and show no interaction with triflate anions. This is in contrast to polymer model **7** complexed with $AgSO_3CF_3$.

However, examination of the data in Table 5 predicts no preferred binding of Ag^+ to specific sites within the polymer. The Ag^+ ions in the model are located throughout the polymer chains and are coordinated to both the sulfur and oxygen atoms of the polymer side chains and

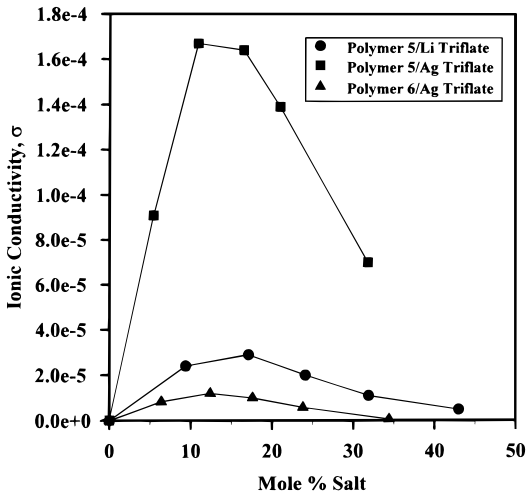

Figure 5. Ionic conductivity of solvent-free polymers **5** and **6** after salt complexation (25 °C).

the nitrogen atoms of the backbone. The ^{13}C NMR shift and T_1 relaxation time data, presented in Figures 2 and 4 and discussed earlier, both suggested preferential coordination of Ag^+ to the sulfur atoms. Furthermore, the ^{15}N natural abundance NMR data suggested no coordination with the backbone nitrogen atoms. Thus, the MD simulations favor a different coordination pattern than is implied by the NMR results.

MD simulations were also carried out in the absence of DMF so that the polymers themselves act as the sole solvent for each of the three models described previously. These models resemble the conditions expected during ionic conduction in a solid polymer electroyte. Examination of models **7** and **8,** both complexed with $AgSO_3CF_3$ in the absence of DMF, revealed no preferred coordination between the Ag^+ and any one of the various oxygen atoms in the polymer side chains. In the case of model **8**, the Ag^+ ions are coordinated to both the oxygen atoms and the sulfur atoms in the polymer side chains. Coordination to the nitrogen atoms in the polymer backbones was again suggested. Thus, similar interactions are predicted whether or not DMF is present. However, this similarity was not evident for the simulation of model **7** complexed with $LiSO_3CF_3$. As described previously, the DMF-solvated model predicts that the Li^+ ions are primarily solvated by DMF molecules with little interaction with the polymer chains. By contrast, the Li^+ ions in the simulated DMF-free polymer−salt complex are highly coordinated to both the oxygen and nitrogen atoms in the polymer with no preferred binding sites existing between the ions and the polymers.

Of special interest was the interaction of the Ag^+ and Li^+ cations with the triflate anions. As mentioned previously, some connection may exist between ion clustering and the mechanism of ion transport in certain polymer electrolytes such as PEO and its derivatives. For solvent-free simulations, both model **7** complexed with $LiSO_3CF_3$ and model **8** complexed with $AgSO_3CF_3$ predicted a greater propensity for ion pairing and clustering than when DMF was present. This tentatively suggests that the clustering of ions may play a greater role in the mechanism of ion transport in polyphosphazene solid polymer electrolytes than in the gel electrolyte systems.

Ionic Conductivity Results. The ionic conductivities of solvent-free salt complexes of polymers **5** and **6** are shown in Figure 5. A similar trend in conductivity

with increasing salt concentration was found for all the polymers. The conductivities increased, reached a maximum, and then decreased. The conductivites of polymer **5** complexed with $LiSO_3CF_3$ or $AgSO_3CF_3$ have been reported previously,[9] and the values observed in this study agreed with those reported earlier. Polymer **5** gave a maximum room temperature (25 °C) ionic conductivity of 2.9×10^{-5} S cm^{-1} when complexed with 17.1 mol % $LiSO_3CF_3$ and 1.67×10^{-4} S cm^{-1} when complexed with 10.9 mol % $AgSO_3CF_3$.

The ionic conductivity was also measured for solvent-free polymer **6** complexed with $AgSO_3CF_3$. This system demonstrated the lowest ionic conductivity of the three complexes measured with a maximum value of 1.2×10^{-5} S cm^{-1} at 12.4 mol % $AgSO_3CF_3$. On the basis of the NMR work, it appears that the lower conductivity of polymer **6** with $AgSO_3CF_3$ than of polymer **5** can be attributed to the presence of the sulfur atoms in the side chains. ^{13}C NMR shifts and T_1 relaxation times for the two carbon atoms chemically bound to the sulfur atom indicated the strongest interaction of the silver ions with the sulfur atoms (although the MD simulations did not predict this). If this interaction reflects coordination strength, then the sulfur atoms are coordinated to the silver ions more strongly than to the oxygens, and transport of the metal ion in a solvent-free system is hindered.

To make a direct comparison of the NMR results to the ionic conductivity of these three systems, conductivity values were also obtained on 1 M polymer solutions in DMF with 12.4 mol % salt (Table 5). These values at room temperature are 1−2 orders of magnitude higher than those for polymers without DMF. Presumably, this is because the solvent molecules become the preferred ion transport medium rather than the polymer. Previous studies on other polymer electrolytes have used DMF as an added plasticizer to enhance conductivity.[19,20] The conductivity of a DMF solution of polymer **5** whether complexed with $LiSO_3CF_3$ or $AgSO_3CF_3$ was found to be 3.0×10^{-3} S cm^{-1}. This is the level of conductivity needed for practical devices. Although it might be expected that the conductivity of polymer **5** with the lithium salt in solution might be higher because of the faster diffusion of the smaller lithium ions through DMF, as well as the preference of DMF for lithium ions, no enhancement of conductivity was detected.

The coordination of silver ions to sulfur atoms reduced the solution conductivity in DMF only slightly. A 1 M solution of polymer **6** in d_7-DMF complexed with $AgSO_3CF_3$ had a conductivity of 2.4×10^{-3} S cm^{-1}.

Thermal Transitions. The glass transition temperatures (T_g's) for solid polymers **5** and **6** were measured by DSC. The DSC curves of the salt-free as well as the salt-complexed polymers confirmed that these materials were completely amorphous over the temperature range of −100 to +75 °C. Polymer **5** has a T_g of −84 °C, which is lower than that of polymer **6** (−70 °C). All three of the solid polymers underwent increases in T_g when salt was added (Figure 6). Metal ions coordinate to the polymer and form ionic cross-links. These cross-links hinder the motion of the polymer side chains, and this is reflected in the T_g.

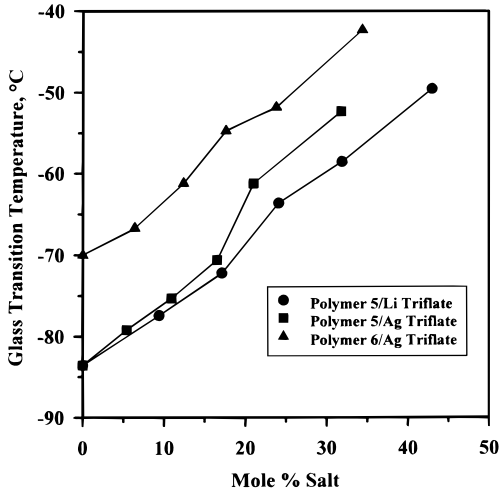

Figure 6. Glass transition temperature of solvent-free polymers **5** and **6** after salt additions.

Conclusions

For all three polymer systems, the experimental ionic conductivities were increased by 1−2 orders of magnitude when DMF was present as a solvent for the polymer and salt, and this undoubtedly reflects the mobility of the DMF-coordinated cations.

The complexes of polymers **5** and **6** with $LiSO_3CF_3$ and $AgSO_3CF_3$ in d_7-DMF were analyzed by ^{13}C, ^{31}P, ^{15}N NMR, and ^{13}C NMR spin−lattice relaxation (T_1) studies as well as through molecular dynamics simulations. The degree of polymer−salt coordination appears to depend on the competing interactions of the salt with the DMF solvent. Lithium ions interact more strongly with DMF than do silver ions. Thus, the ^{31}P and ^{13}C NMR data and the T_1 relaxation times were consistent with a situation in which Li^+ is only weakly bound to the oxygen atoms of the polymer while Ag^+ is bound more strongly to the macromolecule.

Efforts to determine experimentally and computationally which specific coordination sites on the different polymers complexed with the two cations yielded ambiguous results. Analysis of ^{13}C NMR shifts and T_1 relaxation times suggested that Ag^+ ions preferentially bind to the sulfur coordination site of polymer **6**. This conclusion is consistent with the relatively low ionic conductivity of the corresponding solid polymer complex. However, ^{15}N natural abundance NMR indicated that the nitrogen atoms of the backbone of the phosphazene polymers are probably not involved in coordination to either Li^+ or Ag^+ ions, whereas MD simulations on models of the various polymer−salt complexes predicted both coordination to the nitrogen atoms of the polymer backbone and a lack of preference of either cation for any of the coordination sites on polymer **5** or **6**. In the absence of other experimental data, we prefer the model in which the backbone nitrogen atoms do not participate significantly in the coordination behavior, mainly because of the uncertainties inherent in the MD force field development. However, this question could be answered with more certainty by the use of ^{17}O NMR and by solid-state NMR experiments to eliminate the influence of DMF.

Experimental Section

Equipment. ^{1}H (360.0 MHz), ^{13}C (90.0 MHz), and ^{31}P (145.8 MHz) NMR spectra were recorded using a Bruker WM-360 spectrometer with $CDCl_3$, d_8-THF, or d_7-DMF (ISOTEC, Inc.) as the solvent. Chemical shifts are relative to tetramethylsilane at $\delta = 0.00$ ppm for protons and carbon. The phosphorus chemical shifts are relative to external 85% phosphoric acid at $\delta = 0.00$ ppm with positive shift values downfield from the

reference. ^{15}N (50.7 MHz) natural abundance NMR spectra were recorded using a Bruker AMX-2-500 spectrometer with d_7-DMF as the solvent. Spectra were referenced indirectly to ammonia at $\delta = 0.00$ ppm by using a solution of triethylamine at $\delta = 48.2$ ppm in d_7-DMF and were recorded for a maximum period of 24 h. Elemental analyses were obtained by Galbraith Laboratories, Knoxville, TN. Molecular weights were determined through the use of an HP 1090 gel permeation chromatograph equipped with an HP 1047A refractive index detector and two Phenominex Phemgel linear 10 columns. A 0.01 M solution of tetrabutylammonium nitrate in THF was used as the eluting solvent. The injection volume was 10 μL of a 10 mg polymer sample dissolved in 1 mL of THF. Molecular weights are reported versus polystyrene standards. Analysis of the chromatographs was conducted on an HP Chemstation equipped with Polymer Laboratories software. Thermal analyses were carried out with the use of a Perkin-Elmer thermal analysis system 7 equipped with a Perkin-Elmer 7500 computer. For determination of glass transition temperatures by differential scanning calorimetry, heating rates of 10, 20, and 40 °C/min under a nitrogen atmosphere were used, and the values were extrapolated to 0 °C/min. A sample size between 10 and 30 mg was used. Infrared spectra of the polymer−salt complexes were obtained by the use of a Perkin-Elmer 1600 series FT-IR spectrophotometer.

Materials and Procedures. The 2-(2-methoxyethoxy)-ethanol (Aldrich) and the 2-(2-chloroethoxy)ethanol (Aldrich) were purified by vacuum distillation and stored over 4 Å molecular sieves. Hexachlorocyclotriphosphazene (Ethyl Corp./Nippon Fine Chemical) was purified by recrystallization from heptane and by sublimation under vacuum (0.01 mmHg) at 30 °C. Poly(dichlorophosphazene) was prepared by the thermal ring-opening polymerization of the cyclic trimer at 250 °C. All substitution reactions were carried out under an atmosphere of dry argon (Matheson) with the use of standard Schlenk line and drybox techniques. Tetrahydrofuran (Omnisolv) was dried over sodium benzophenone ketyl and was distilled under an argon atmosphere. Lithium triflate (Aldrich) and silver triflate (Aldrich) were dried under vacuum (0.01 mmHg) at 60 °C for 2 days and stored under vacuum.

***T*$_1$ Measurements.** All samples were dissolved to yield 1 M solutions of polymer in d_7-DMF. These were then degassed through a freeze−pump−thaw cycle (3×) and sealed under vacuum. An inversion recovery pulse sequence was used to make all T_1 measurements in the liquid state. T_1 values were calculated with Bruker T_1 software which uses an exponential least-squares data fitting method.

Two-Dimensional Experiments. Two-dimensional $^{13}C-^{1}H$ correlations were carried out in the inverse mode on a Bruker AM300 spectrometer using a modified HMQC experiment[57] with GARP-1 decoupling[59] in which a BIRD sequence[60] was used to suppress ^{1}H signals from protons not directly coupled to ^{13}C.

MD Simulation Protocol. MD simulations were carried out using a modified parallelized version of the SANDER module from AMBER 4.1[61] running on the Cray-T3D at the Pittsburgh Supercomputing Center. The system was held at 300 K by using separate temperature coupling for the polymer and the solvent.[62] The simulations were completed using a 1.5 fs time step in conjunction with SHAKE to constrain all bonds.[63] Constant pressure periodic boundary conditions were employed with a cutoff distance of 10 Å for nonbonded interactions. Electrostatic and van der Waals interactions beyond the cutoff distance were accounted for by using Ewald sums and van der Waals long-range correction terms.[64,65] For the Ewald sums, a real space decay factor of $\alpha = 0.39$ and a maximum reciprocal space vector $k_{max} = 10$ were used. This corresponds to a total of 2280 independent k vectors for the calculation of the reciprocal space contribution. The models described above were slowly equilibrated by simulating temperature increases in several steps (0−100 K for 15 ps, 100−200 K for 15 ps, and 200−300 K for 15 ps) to 300 K. Full equilibration runs were performed until the periodic box dimensions were stabilized (approximately 150 ps). The total simulation time was 500 ps with atomic coordinates being collected every 50 steps.

Conductivity Measurements. Polymers **5** and **6** were stored in an argon atmosphere glovebox until needed. Solutions of the polymers and salts were made up in *N*,*N*-dimethylformamide (J.T. Baker), the solvent was removed, and the complexes were initially dried at 55 °C under vacuum (0.01 mmHg) for 3 days and then at 0.01 mmHg and 25 °C for 2 days. The absence of *N*,*N*-dimethylformamide from the complexes was indicated by infrared spectroscopy. Samples were placed between platinum blocking electrodes and were supported by a Teflon O-ring. They were then placed in a fixture to which leads were attached. Conductivity measurements on solid polymer−salt complexes were carried out with the use of a Hewlett-Packard 4192A LF impedance analyzer set at an ac potential of 1 V with complex impedance techniques used over a frequency range of 5 Hz to 13 MHz. Measurements were taken under a constant flow of argon atmosphere at 25 °C (±2 °C). Conductivity measurements on the 1 M solutions of polymer−salt complexes were carried out with the use of a Coulter DELSA 440SX. Measurements were taken at 25 ± 1 °C.

Synthesis of 2-(2-Methylthioethoxy)ethanol (2). A reaction flask containing sodium methanethiolate (10 g, 0.143 mol) (Fluka) in dry dioxane (400 mL) was warmed gently. To this warm solution was added 2-(2-chloroethoxy)ethanol (11.88 g, 0.095 mol) (Aldrich) over a period of an hour. The reaction mixture was stirred and heated at reflux for 12 h. After this time, the mixture was cooled to ambient temperature, and distilled water (100 mL) was added to dissolve the salts formed. The solution was extracted four times with chloroform. The organic fractions were combined and dried over $MgSO_4$. The drying agent was removed by filtration, and the solvent was removed by rotary evaporation. A pale yellow oil remained, which was distilled under reduced pressure (70−75 °C, 0.05 mmHg) to yield a clear, colorless liquid. Yield: 82%, 10.59 g, 0.078 mol. ^{1}H NMR ($CDCl_3$), δ (ppm): 2.13 (s, 3H), 2.40 (t, 1H), 2.69 (t, 2H), 3.57 (t, 2H), 3.66 (t, 2H), 3.68 (q, 2H). ^{13}C NMR ($CDCl_3$), δ(ppm): 15.97, 33.72, 61.72, 70.01, 72.01. Mass spectrometry, *m*/*e*: 137 MH+ base peak.

Synthesis of Poly[bis(2-(2-methoxyethoxy)ethoxy)]-phosphazene (5). 2-(2-Methoxyethoxy)ethanol (34.24 g, 0.285 mol) (Aldrich) was added to sodium metal (7.20 g, 0.314 mol) in dry tetrahydrofuran (500 mL). This solution was heated gently, and once the sodium salt had formed, to this was added dropwise a solution of poly(dichlorophosphazene) (11.00 g, 0.095 mol) in dry tetrahydrofuran (600 mL) under an atmosphere of argon over a period of 2 h. The reaction mixture was stirred and refluxed for 24 h under argon. Immediately after the heating was terminated the mixture was filtered and the filtrate concentrated by removal of the solvent through rotary evaporation. The concentrated residue was dialyzed against distilled−deionized water (1 week) and then methanol (1 week). The solvent was removed through rotary evaporation, and the remaining material was further dried at 50 °C under reduced pressure (0.1 mmHg) for 2 days. The final product, polymer **5**, was obtained as a clear, pale yellow gum. Yield: 60%, 16.13 g, 0.057 mol. ^{31}P NMR (d_7-DMF), δ (ppm): −7.29. ^{1}H NMR ($CDCl_3$), δ (ppm): 3.35 (s, 3H), 3.51 (t, 2H, 3.62 (m, 4H), 4.05 (t, 2H). ^{13}C NMR (d_7-DMF), δ (ppm): 58.67, 65.66, 70.69, 70.85, 72.40. ^{15}N NMR (d_7-DMF), δ (ppm): 64.0. GPC: $M_w = 1.7 \times 10^5$. DSC: $T_g = -83$ °C. Elemental analysis calculated: C, 42.4%; H, 7.8%; N, 4.9%. Found: C, 42.1%; H, 7.3%; N, 4.5%.

Synthesis of Poly[bis(2-(2-methoxythioethoxy)ethoxy-)]phosphazene (6). Polymer **6** was prepared as described for polymer **5**. The reagents and quantities used were as follows: poly(dichlorophosphazene) (11.00 g, 0.095 mol), 2-(2-methylthioethoxy)ethanol (38.76 g, 0.285 mol) (**2**), sodium metal (7.2 g, 0.314 mol), and dry tetrahydrofuran (1.1 L). The polymer was purified by precipitation into distilled−deionized water (3×) and hexane (3×). The final product, polymer **6**, was dried at 50 °C under reduced pressure (0.01 mmHg) for 2 days. Yield: 68%, 20.35 g, 0.065mol. ^{31}P NMR (d_7-DMF), δ (ppm): −7.26. ^{1}H NMR (d_7-DMF), δ (ppm): 2.18 (s, 3H), 2.74 (t, 2H),

3.72 (m, 4H), 4.17 (t, 2H). ^{13}C NMR (d_7-DMF), δ (ppm): 15.92, 33.81, 65.70, 70.64, 71.06. ^{15}N NMR (d_7-DMF), δ (ppm): 64.0. GPC: $M_w = 4.8 \times 10^5$. DSC: $T_g = -70$ °C. Elemental analysis calculated: C, 38.1%; H, 7.0%; N, 4.4%. Found: C, 37.6%; H, 6.6%; N, 4.7%.

Acknowledgment. The work was supported by the Department of Energy through Grant No. DE-FG02-93ER14387.

References and Notes

(1) (a) Fenton, D. E.; Parker, J. M.; Wright, P. V. *Polymer* **1973**, *14*, 589. (b) Wright, P. V. *Polym. J.* **1975**, *7*, 319.
(2) (a) Armand, M. B.; Chabagno, J. M.; Duclot, M. J. *Abstracts of Papers*, Second International Meeting on Solid Electrolytes, St. Andrews, Scotland, 1978. (b) Armand, M. B.; Chabagno, J. M.; Duclot, M. J. In *Fast Ion Transport in Solids*; Duclot, M. J., Vashishta, B., Mundy, J. N., Shenoy, G. K., Eds.; North-Holland: Amsterdam, 1979. (c) Berthier, C.; Gorecki, W.; Minier, M.; Armand, M. B.; Chabagno, J. M.; Rigaud, P. *Solid State Ionics* **1983**, *11*, 91.
(3) Shriver, D. F.; Farrington, G. C. *Chem. Eng. News* **1985**, *63* (20), 42.
(4) Ratner, M. A.; Shriver, D. F. *Chem. Rev.* **1988**, *88*, 109.
(5) Bruce, P. G.; Vincent, C. A. *J. Chem. Soc., Faraday Trans.* **1993**, *89* (17), 3187.
(6) Allcock, H. R.; Kugel, R. L. *J. Am. Chem. Soc.* **1965**, *87*, 4216.
(7) Allcock, H. R.; Kugel, R. L.; Valan, K. J. *Inorg. Chem.* **1966**, *5*, 1709.
(8) Allcock, H. R.; Kugel, R. L. *Inorg. Chem.* **1966**, *5*, 1716.
(9) Blonsky, P. M.; Shriver, D. F.; Austin, P.; Allcock, H. R. *Solid State Ionics* **1986**, *18/19*, 258.
(10) Blonsky, P. M.; Shriver, D. F.; Austin, P.; Allcock, H. R. *J. Am. Chem. Soc.* **1984**, *106*, 6854.
(11) Blonsky, P. M.; Shriver, D. F.; Austin, P.; Allcock, H. R. *Polym. Mater. Sci. Eng.* **1985**, *53*, 118.
(12) Lerner, M. M.; Tipton, A. L.; Shriver, D. F.; Dembek, A. A.; Allcock, H. R. *Chem. Mater.* **1991**, *3*, 1117.
(13) Lerner, M. M.; Lyons, L. J.; Tonge, J. S.; Shriver, D. F. *Chem. Mater.* **1989**, *1*, 601.
(14) a. Allcock, H. R.; Kuharcik, S. E.; Reed, C. S.; Napierala, M. E. *Macromolecules* **1996**, *29*, 3384−3389. (b) Allcock, H. R.; O'Connor, S. J. M.; Olmeijer, D. L.; Napierala, M. E.; Cameron, C. G. *Macromolecules* **1996**, *29*, 7544.
(15) Allcock, H. R.; Ravikiran, R.; O'Connor, S. J. M. *Macromolecules* **1997,** *30*, 3194.
(16) Ratner, M. A.; Shriver, D. F. *Chem. Rev.* **1988**, *88*, 109.
(17) Vincent, C. A. *Electrochim. Acta* **1995**, *28*, 5312.
(18) Disssanayake, M. A. K. L.; Frech, R. *Macromolecules* **1995**, *28*, 5312.
(19) Forsyth, M.; MacFarlane, D. R.; Meakin, P.; Smith, M. E.; Bastow, T. J. *Electrochim. Acta* **1995**, *40* (13−14), 2343.
(20) Ward, I. M.; Boden, N.; Cruickshank, J.; Leng, S. A. *Electrochim. Acta* **1995**, *40* (13−14), 2071.
(21) Donoso, J. P.; Bonagamba, T. J.; Panepucci, H. C.; Oliveira, L. N.; Gorecki, W.; Berthier, C.; Armand, M. B. *J. Chem. Phys.* **1993**, *98* (12), 10026.
(22) Xie, L.; Farrington, G. C. *Solid State Ionics* **1993**, *60*, 19.
(23) Forsyth, M.; Payne, V. A.; Ratner, M. A.; deLeeuw, S. W.; Shriver, D. F. *Solid State Ionics* **1992**, *53−56*, 1011.
(24) Nazri, G.; MacArthur, D. M.; Ogara, J. F. *Chem. Mater.* **1989**, *1*, 370.
(25) Greenbaum, S. G.; Adamic, K. J.; Pak, Y. S.; Wintersgill, M. C.; Fontanella, J. J. *Solid State Ionics* **1988**, *28−30*, 1042.
(26) Adamic, K. J.; Greenbaum, S. G.; Abraham, K. M.; Alamgir, M.; Wintersgill, M. C.; Fontanella, J. J. *Chem. Mater.* **1991**, *3*, 534.
(27) Liu, K. J. *Macromolecules* **1969**, *2*, 235.
(28) Krajewski-Bertrand, M. A.; Laupretic, F.; Monneric, L. In *Dynamics of Solutions and Fluid Mixtures by NMR*; Delpuech, J. J., Ed.; John Wiley and Sons Ltd.: West Sussex, England, 1995.
(29) Forsyth, M.; Meakin, P. M.; MacFarlane, D. R. *Electrochim. Acta* **1995**, *40* (13−14), 2339.
(30) Greenburg, M. S.; Bodner, R. L.; Popov, A. I. *J. Phys. Chem.* **1973**, *77* , 2449.
(31) Gutmann, V.; Wychera, E. *Inorg. Nucl. Chem. Lett.* **1966**, *2*, 257.
(32) Marcus, Y. In *Ion Solvation*; John Wiley and Sons Ltd.: West Sussex, England, 1985.
(33) Perron, J.; Beauchamp, A. L. *Inorg. Chem.* **1984**, *23*, 2853.
(34) Schmidt, E.; Hourdakis, A.; Popov, A. *Inorg. Chim. Acta* **1981**, *52*, 91.
(35) Petersen, S. B.; Led, J. J.; Johnston, E. R.; Grant, D. M. *J. Am. Chem. Soc.* **1982**, *104*, 5007.
(36) Shamnsipur, M.; Popov, A. I. *J. Am. Chem. Soc.* **1979**, *101*, 4051.
(37) Echegoyen, L.; Kaifer, A.; Durst, H. D.; Gokel, G. W. *J. Org. Chem.* **1984**, *49*, 688.
(38) Izatt, R. M.; Lamb, J. D.; Asay, R. E.; Maas, G. E.; Bradshaw, J. S.; Christensen, J. J. *J. Am. Chem. Soc.* **1977**, *99*, 6134.
(39) Izatt, R. M.; Bradshaw, J. S.; Nielson, S. A.; Lamb, J. D.; Christensen, J. J. *Chem. Rev.* **1985**, *85*, 271.
(40) Izatt, R. M.; Terry, R. E.; Hansen, L. D.; Avondet, A. G.; Bradshaw, J. S.; Dalley, N. K.; Jensen, T. E.; Christensen, J. J. *Inorg. Chim. Acta* **1978**, *30*, 1.
(41) Harris, R. K., Mann, B. E., Eds. *NMR and the Periodic Table*; Academic Press: New York, 1978.
(42) Spindler, R.; Shriver, D. F. *Macromolecules* **1988**, *21*, 3036.
(43) Jorgensen, W. L.; Swenson, C. J. *J. Am. Chem. Soc.* **1985**, *107*, 569.
(44) Catlow, C. R. A.; Mills, G. E. *Electrochim. Acta* **1995**, *40*, 1057.
(45) Vincent, C. A. *Electrochim. Acta* **1995**, *40*, 2035.
(46) Stewart, J. J. P. *J. Comput. Chem.* **1989**, *10*, 209.
(47) Stewart, J. J. P. *J. Comput. Chem.* **1989**, *10*, 221.
(48) MOPAC 6.0 QCPE: Stewart, J. J. P. Indiana University, Bloomington, IN 47405, 1990.
(49) Besler, B. H.; Merz, Jr., K. M.; Kollman, P. A. *J. Comput. Chem.* **1990**, *11*, 431.
(50) Merz, Jr., K. M. *J. Comput. Chem.* **1992**, *13*, 749.
(51) Bayley, C. I.; Cieplak, P.; Cornell, W. D.; Kollman, P. A. *J. Phys. Chem.* **1993**, *97*, 10269.
(52) Removal of the capping groups in this model for **9** and **10** generated a nonintegral total charge (−0.05*e*). Because it is undesirable to allow a partial negative charge on what should be a neutral polymer, the charge on the phosphorus atoms (the least accessible atoms to other atoms and molecules) was modified. This also resulted in the smallest overall charge (∼1.2 → 1.25). This procedure is not unusual in developing force fields for biopolymers.
(53) Gejji, S. P.; Hermansson, K.; Lindgren, J. *J. Phys. Chem.* **1993**, *97*, 3712.
(54) Cornell, W. D.; Cieplak, P.; Bayly, C. I.; Gould, I. R.; Merz, Jr., K. M.; Ferguson, D. F.; Spellmeyer, D. C.; Fox, T.; Caldwell, J. W.; Kollman, P. A. *J. Am. Chem. Soc.* **1995**, *117*, 5179.
(55) Laaksonen, A.; Kovacs, H. *Can. J. Chem.* **1994**, *72*, 2278.
(56) Boyd, R. H.; Kesner, L. *J. Am. Chem. Soc.* **1977**, *99*, 4248.
(57) Allcock, H. R. *Phosphorous-Nitrogen Compounds; cyclic, linear, and high polymeric systems*; Academic Press: New York, 1972.
(58) Summers, M. F.; Marzilli, L. G.; Bax, A. *J. Am. Chem. Soc.* **1986**, *108*, 4825.
(59) Shaka, A. L.; Barber, P. B.; Freeman, R. *J. Magn. Reson.* **1985**, *64*, 547.
(60) Garbow, J. R.; Weitekamp, D. P.; Pines, A. *Chem. Phys. Lett.* **1982**, *93*, 504.
(61) Damodaran, K. V.; Cheng, A.; Merz, Jr., K. M. To be published.
(62) Berendsen, H. J. C.; Postma, J. P. M.; Gunsteren, W. F. v.; DiNola, A. D.; Haak, J. R. *J. Chem. Phys.* **1984**, *81*, 3684.
(63) Ryckaert, J. P.; Ciccotti, G.; Berendsen, H. J. C. *J. Comput. Phys.* **1977**, *23*, 327.
(64) Brown, D.; Neyertz, S. *Mol. Phys.* **1995**, *84*, 577.
(65) Allen, M. P.; Tildesley, D. J. *Computer Simulations of Liquids*; Oxford University Press: New York, 1994; p 385.

MA980665+